



Friction role in bending behaviors of thin-walled tube in rotary-draw-bending under small bending radii

H. Yang*, H. Li, M. Zhan

School of Materials Science, State Key Laboratory of Solidification Processing, Northwestern Polytechnical University, Xi'an 710072, PR China

ARTICLE INFO

Article history:

Received 24 February 2010

Received in revised form 5 August 2010

Accepted 22 August 2010

Keywords:

Friction role
Friction test
Tube bending
Bending deformation
Small bending radii

ABSTRACT

For contact dominated rotary-draw-bending (RDB) of thin-walled tube, friction role should be focused to achieve precision bending under small bending radii ratio ($R_d/D < 2.0$, R_d -bending radius, D -tube diameter). By using explicit FE simulation combined with physical experiment, underlying effects of the friction on bending behaviors are explored from multiple aspects such as wrinkling, wall thickness variation and cross-section deformation. The results show that: (1) By using a simulative twist compression test (TCT), the dynamic contact conditions of RDB with large slipping are reproduced, and the coefficients of the friction (CoFs) under various tribological conditions in RDB are estimated, which provides physical basis for understanding friction role and boundary conditions for FE simulation. (2) Both positive and negative effects of friction role are observed since the friction on each interface affects the multi-defect with different or even contrary tendencies. The effect sensitivity on wrinkling is less obvious than that on wall thinning and cross-section deformation. Under smaller R_d/D , the bending becomes more sensitive to the friction conditions. (3) Considering the knowledge about friction role on individual interface of RDB, by changing two decisive parameters affecting the CoFs such as lubricant types and tube/tool materials, an optimal strategy is proposed to apply the tribological conditions and thus the stable and accurate bending conditions are established for precision forming of RDB under smaller R_d/D .

© 2010 Elsevier B.V. All rights reserved.

1. Introduction

Among various bending methods, due to high efficiency/precision advantages and satisfying large strength/weight ratio needs, the flexible and incremental numerical controlled rotary-draw-bending (RDB) has become one of advanced and universal methods to form thin-walled bent tube components ($D/t > 20$, t -wall thickness) with tight bending radius, which has attracted increasing applications in many industries including aerospace, aviation and automobile (Yang et al., 2006). As shown in Fig. 1, the RDB is a tri-nonlinearity physical process with multi-factor coupling effect and multiple defects such as local wrinkling, over thinning (even crack) and cross-section distortion with the inappropriate forming parameters applied. Compared with other bending processes, RDB is a contact dominant process under multi-die constraints including bend die, clamp die, pressure die, wiper die and mandrel (with mandrel shank and flexible balls). Only under precision cooperation of these tools, may the stable and precision bending deformation be achieved under small R_d/D , viz., free wrinkling, allowed wall thinning and cross-section deformation degrees. As a major factor affecting the contact conditions,

the friction on various tube–tool interfaces may play considerable effect on bending deformation behaviors of RDB.

Up to now, many researchers have studied tube bending via experimental, analytical or numerical methods, however, most focus on pure bending, rolling bending, stretch bending or press bending. These studies provide useful knowledge for bending behaviors of thin-walled tube bending (TWTB). In the last two decades, the study on RDB has been reported, in which the effects of basic forming parameters such as geometrical and material properties on bending were investigated in terms of individual defect. Welo et al. (1994) proved that FE analysis can be a well-suited numerical tool for design and product optimization in RDB with dynamic boundary conditions. Yang et al. (2001) numerically studied the effect of bending radius and tube thickness on cross-section deformation and wall thinning. Trana (2002) found that the bending deformation should be considered in hydroforming simulation to obtain reliable prediction results. However, in the above literature, for relatively thick-walled tube bending with large R_d/D was considered, the various defects of bending tube can be easily avoided by changing the processing parameters with some accumulated experiences, thus the friction role in tube bending was generally neglected.

However, under tough forming conditions under smaller R_d/D , which is currently urgently needed in many industries, the bending tube deforms more unevenly and the multi-defect become

* Corresponding author. Tel.: +86 29 88495632; fax: +86 29 88495632.

E-mail addresses: yanghe@nwpu.edu.cn (H. Yang), liheng@nwpu.edu.cn (H. Li).

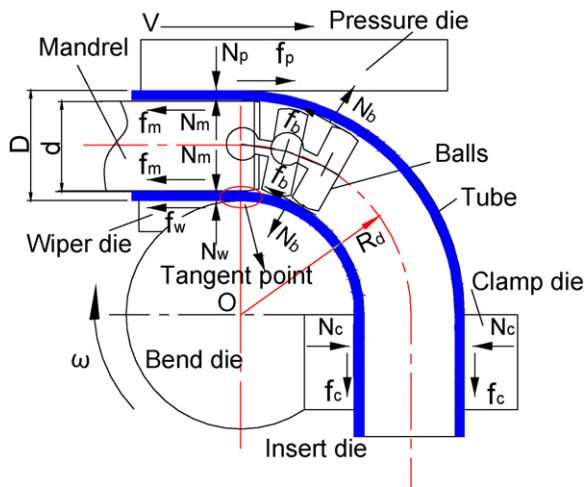


Fig. 1. Schematic diagram of RDB and friction force.

more prone to occur (Lowery, 2008). Thus to obtain the precision bending of thin-walled tube, for given tube material and bending specification, the treatment of the friction conditions on various interfaces should be preliminarily concentrated to ensure stable bending loading since the effects of the other forming parameters on bending tube are all standing on the tribological conditions. While, due to lack of knowledge on friction role in bending of RDB for thin-walled tube, in practice, the tribological conditions cannot be treated consciously and properly, and the “trial and error” is still mainly used to optionally apply lubricants with inferior repeatability, though some prior observations on friction effect in tube bending were carried out.

Oliveira et al. (2005) assessed the lubricant performance experimentally in tube bending of steel/aluminum tubes, and found that the mandrel load, surface quality and thinning degree of bending tube were manifestly affected by the lubricant type. While more quantitative study on friction role and underlying mechanism of bending behaviors cannot be conducted by the experiment because of the complexity of the RDB. Either, the analytical results far deviate from the experimental ones since the friction conditions on various interfaces are difficult to be considered in the formulas (Tang, 2000). Nowadays, 3D FE simulation has been proved to be the primary approach to probe the deformation behaviors of RDB with complicated contact conditions (Li, 2007). By using FE simulation, Yang et al. (2009) found that with the larger the diameter of bending tube, the larger the effects of friction between tube and dies on wrinkling tendency. However, in most reported FE modeling, the coefficients of friction (CoFs) on all different tube–die interfaces are designed as 0.1 or no friction is assumed without robust physical foundation. For RDB with highly nonlinear dynamic conditions, the friction role on bending behaviors should be quantitatively and efficiently addressed by using 3D-FE explicit simulation (ABAQUS, 2005) via considering multiple defects such as wrinkling, wall thickness variation and cross-section distortion.

The present study attempts to obtain the epistemological understanding of the friction role in bending deformation of RDB with respect to multiple defects. Firstly, among many physical friction tests (Bay et al., 2008), such as strip drawing test, deep drawing test, strip tension test, etc., the TCT is selected to reproduce the friction conditions of RDB and evaluate the CoFs for various tribological conditions. Then via 3D-FE simulation and experiment, a systematic study on friction effects on bending deformation on different interfaces is conducted in terms of various defects. Finally, an optimal strategy is proposed to actively treat the tribological issues

for RDB to establish a sound preliminary forming condition and improve the bending forming quality, as well as reduce the wear of tools.

2. Experimental procedure for friction evaluation

The friction characteristics and the CoFs under various tribological conditions are addressed and estimated by the experimental test of TCT.

2.1. Contact interfaces and friction features in RDB

During RDB, as shown in Fig. 1, the pressure force N_c is applied to the front end tube by the insert die (tied with bend die) and clamp die, which exerts enough friction force f_c and helps drag the tube past the tangent point and rotate along the groove of bend die. Thus the designed bending radius R_d and bending angle could be achieved. Pressure die exerts the pressure force N_p to half outer surface of tube against wiper die, which provides bending torque and applies the forward friction force f_p to the tube to help push the materials into the deformation areas. Besides the above basic tools for tube bending, both the mandrel and wiper die are used to exert normal force N_m , N_b and N_w to restrain wrinkling and reduce cross-section deformation. While they induce friction force f_m , f_b and f_w with contrary direction to tube forward flow.

Thus in RDB, the deformation of tube depends on the contact conditions between tube and various dies, which may change local or the whole stress/strain distributions of bending tube. Altogether, there are five interfaces involved in thin-walled bending including tube–wiper die, tube–mandrel (including tube–balls), tube–pressure die, tube–bend die and tube–clamp die. Based on the above analysis, it is thought that, except for tube–clamp die interface, there is finite relative slip between tube and dies, such as tube–wiper die, tube–mandrel, tube–pressure die and tube–bend die. Then the friction types on these interfaces can be viewed as kinetic ones. Also the local progressive bending feature in RDB results in almost constant contact areas on friction interface.

2.2. Friction evaluation by using TCT

To explore the friction conditions and obtain the CoFs of sheet metal–tool interfaces, several methods have been reviewed and proposed (Bay et al., 2008). These methods can be classified into simulative and process tests. As mentioned in Section 2.1, the tube is supported by both external and internal tools in RDB. Thus the process test cannot be used to evaluate the CoFs on various contact interfaces. Meanwhile, among common simulative tests, the TCT is more suitable for CoF estimate by its unique procedure, in which, normal pressure is combined with continued sliding over the same surface area by rotation of a die or the specimen (Kim et al., 2008). Since several variables such as tube material, tool material, types of lubricant, pressure force and large rotate speed can be varied under dynamic contact conditions while remaining a constant contact area, the TCT is used to reproduce the dynamic contact conditions of RDB.

Fig. 2 shows a device of the TCT and corresponding samples. In this friction test, an annular cylinder specimen is lowered under hydraulic pressure and contacted with a flat specimen, which is retained in a horizontal position. Then the annular specimen is rotated with constant speed against the flat one. The flat specimen is polished with the same materials as tube materials; while the upper cylinder is made with the same ones with tools in tube bending. Then this test measures the transmitted torque between rotating cylinder and the lubricated flat specimen. The friction twist torque T is then transferred to the friction force F . According to the

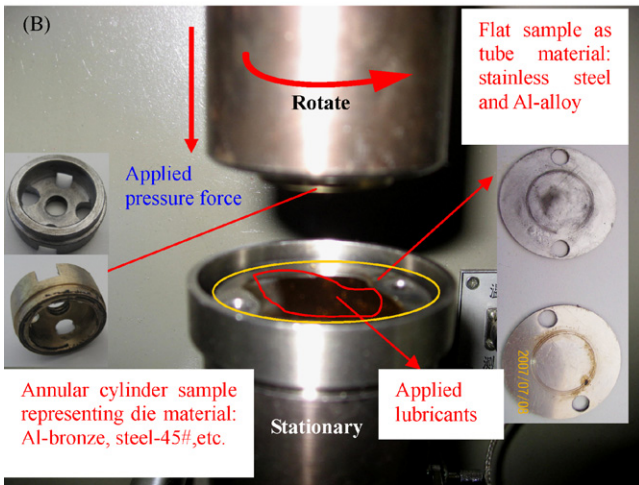
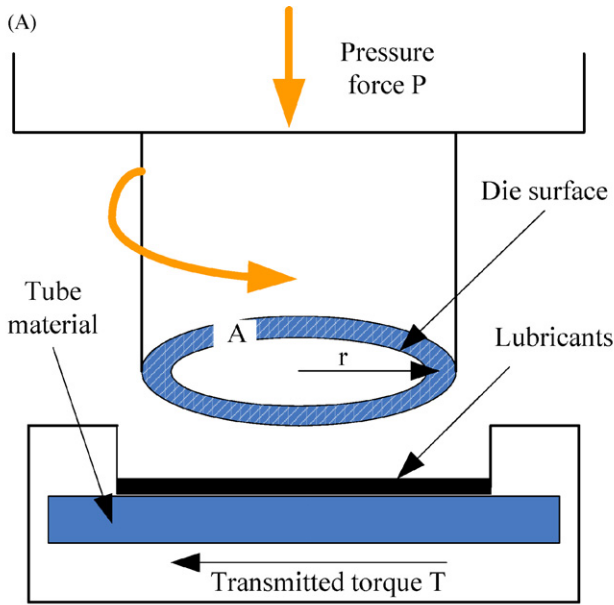


Fig. 2. TCT friction test (a) schematic of TCT; (b) setup of TCT.

Coulomb law, one suitable theoretical model in sheet metal forming (Joun et al., 2009), the CoF is then calculated from the ratio of transmitted torque F to applied pressure P as Eq. (1):

$$\mu = \frac{F}{P} = \frac{T}{PrA} \quad (1)$$

where r is the mean radius of the tool, A is the cross-sectional area of the tool.

By changing the combinations of the tube materials/die materials/kinds of lubricants employed in RDB, the rotate speed and the pressure force, the TCT test is conducted at room temperature.

The available lubricant is extrusion oil S980B, aviation oil and MoS_2 . Both the S980B and aviation oil are highly viscous fluid lubricants with good oiliness; MoS_2 is a solid lubricant. Three lubricant conditions are applied: DF (dry friction), tough DF (placing hard abrasive sandpaper with no lubricant) and lubricated. The tube material is Al-5052O, stainless steel-1Cr18Ni9Ti and medium strength Ti-alloy TA18M. The tool materials are steel-45#, Al-bronze and Cr12MoV. The blasting with sand of different roughness is applied to polish the working surface of the tools and obtain different surface roughness degrees. The roughness degree of the tube materials is 0.5–0.6 μm , and the ones of the steel-45#

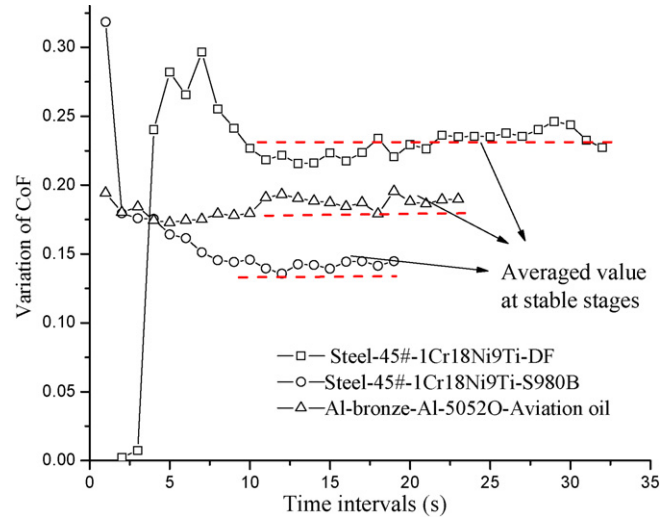


Fig. 3. The average values of CoFs at stable periods of TCT under different tribological conditions.

tool, Al-bronze and Cr12MoV are 2.5–3.2, 0.8–1.2 and 0.5–0.9 μm , respectively. Especially, the other two roughness degrees, viz., 2.2–2.8 and 4.1–4.6 μm , are obtained to study the roughness's effect on CoFs. As shown in Fig. 3, the average values of CoF under different dynamic boundary conditions are estimated and the friction behavior can thus be addressed.

Fig. 4 shows that, the lubricant kinds and their application have significant effect on the magnitude of the CoF values. Under DF condition, the CoF is much larger than that under lubricated conditions. With the lubricants of S980B and aviation oil, the CoFs are relatively smaller and more stable during the test than that with MoS_2 . Besides the kinds of the lubricants, the tube material/die surface combinations also have greater effect on the variation of the CoF values. It shows that, with S980B or aviation oil lubricants applied, the CoFs are relatively smaller for steel-45#-Al-5052O, Al-bronze-1Cr18Ni9Ti and Cr12MoV-Al-5052O. It is noted that, for the TA18M, the CoFs with different tool materials including Cr12MoV and Al-bronze are estimated. The result confirms that the different combination of tube and tool materials should be paid most attention in friction design process of tube bending. Also, it shows that, in the current scope, the value of the CoF increases greatly with larger roughness degrees under DF conditions; while the value of the CoF varies a little with larger surface roughness under lubricant conditions.

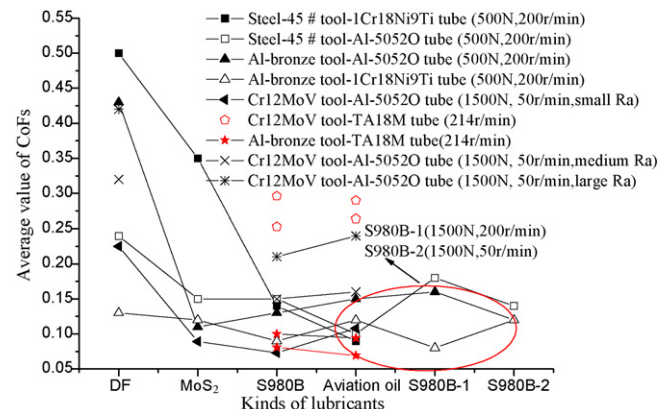


Fig. 4. The average values of CoFs under different tube material/lubricant/die surface combination conditions.

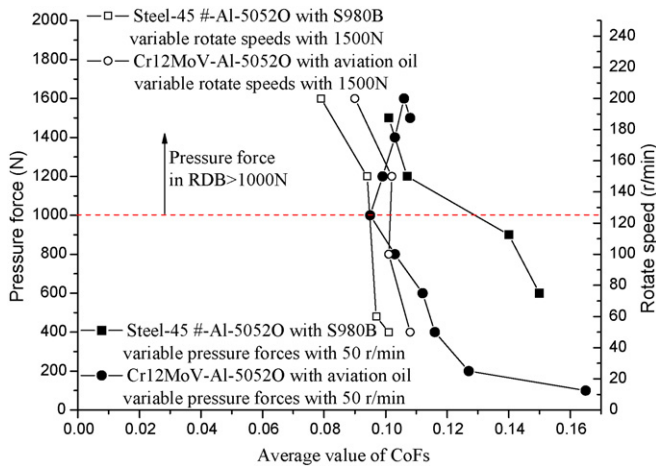


Fig. 5. The average values of CoFs under different tube material/lubricant/die surface combination conditions.

Compared with the values under different tube materials/tool materials/lubricant combinations (including surface roughness), the CoFs varies relatively little with pressure force or rotate speed changed as shown in Fig. 5, though the CoFs decrease with increasing the sliding velocity and normal load, which was also observed in literature for Al-6061(T4)–nature rub interface (Ramezani et al., 2009). With different rotate speeds, the average value of CoF is 0.09 with maximum positive deviation of 8.6% and maximum negative deviation of 15.1%; with changing of the pressure die, the average CoF value is 0.12 with maximum positive deviation of 17.6% and maximum negative deviation of 12%.

Then by using the TCT, the following assumptions can be made to help model the friction behavior in 3D-FE simulations: (1) The decisive parameters related to the CoF are kinds of lubricant, tube materials and tool materials as well as surface treatment. Relatively, the pressure force and rotate speed (sliding velocity) can be viewed as neglected factors. (2) The CoF under finite dynamic friction conditions can be regarded as invariable in RDB.

Table 1

Mechanical properties of tube materials used in FE model.

Materials	Al-5052O	1Cr18Ni9Ti
Fracture elongation (%)	22	60.3
Poisson's ratio	0.34	0.28
Initial yield stress (MPa)	90	213
Hardening exponent n	0.262	0.54
Strength coefficient K (MPa)	431	1591
Young's modulus (GPa)	56	200
Density (kg/m^3)	2700	7800
Anisotropy exponent	0.55	0.94

3. 3D-FE model of RDB and experimental validation

Under FE platform ABAQUS (2005), an elastic–plastic 3D-FE model is established to simulate RDB of thin-walled tube. As shown in Fig. 6, a half model of tube bending $50 \times 1 \times 75$ mm ($D \times t \times R_d$) is developed to reduce the computation cost.

The explicit algorithm is used for tube bending and balls retracting operation; while the implicit one is employed for unloading process (springback). As shown in Fig. 6, the boundary constraints are applied by two approaches to realize the actual process of RDB: 'displacement/rotates' and 'velocity/angular'. Both bend die and clamp die are constrained to rotate about the global x -axis simultaneously; pressure die is constrained to translate only along the global z -axis; wiper die is constrained along all degrees of freedom; the mandrel (including mandrel shank and multi-balls) is kept stationary along z -axis during bending, while the mandrel is retracted with the bending deformation is finished; the 'connector element' is used to define the 'hinge' contact behaviors between mandrel shank and flexible balls. The trapezoidal profile is used to define the smooth loading of all the above tools to reduce inertial effects in explicit simulation of the quasi-static process.

The strain hardening characteristics is described by $\bar{\sigma} = K\bar{\epsilon}^n$ and the Hill's anisotropic quadratic yield function is used to describe tube material's yield behaviors. Table 1 shows the mechanical properties of the tube materials obtained by the uniaxial tension test, in which the arc specimen was directly cut out from the tube along the longitudinal direction by wire cut. The level of equivalent strain during bending is higher than the maximum level of equivalent

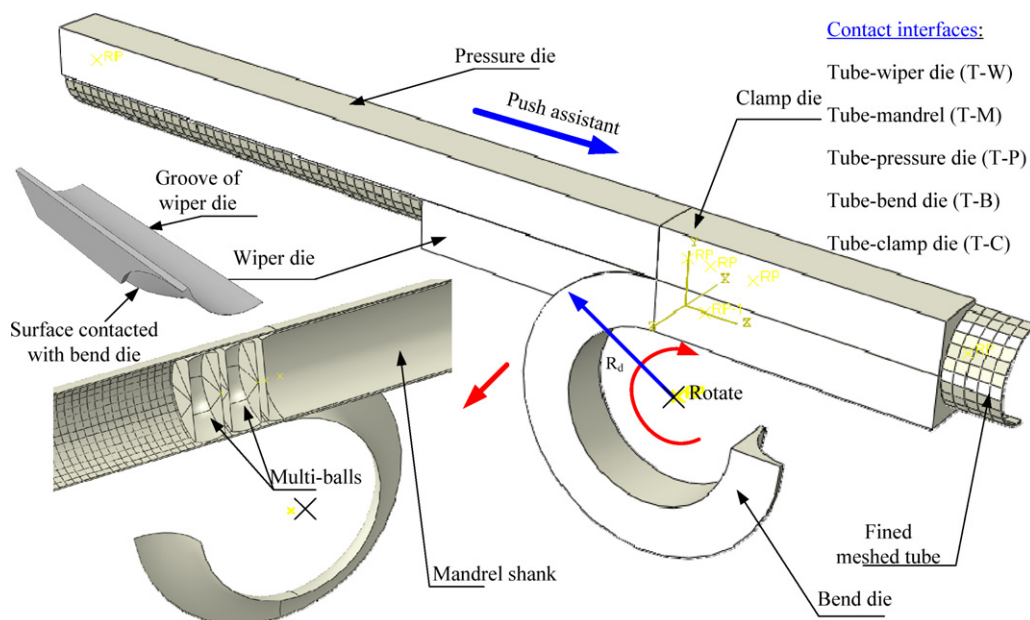


Fig. 6. Diagram of 3D-FE half model of TWBTB $50 \times 1 \times 75$.

Table 2
CoFs on various contact interfaces and related setting in FE simulation.

	Contact interfaces	CoFs	Formulation of the mechanical constraints	Lubricant conditions
1	Tube–wiper die	0.15	Kinematic method-finite sliding	Lubricated
2	Tube–pressure die	0.45	Kinematic method-finite sliding	DF
3	Tube–clamp die	0.6 or rough	Kinematic method-small sliding	Tough DF
4	Tube–bend die	0.15	Kinematic method-finite sliding	DF
5	Tube–mandrel	0.1	Kinematic method-finite sliding	Lubricated
6	Tube–balls	0.1	Penalty method-finite sliding	Lubricated

strain obtained in the tension test, so the remaining part of the flow curve is extrapolated for the FE simulation. The tube is meshed with four-node doubly curved thin shell S4R; the relative rigid tools are modeled with four-node bilinear quadrilateral rigid element R3D4. The element size 3×3 mm is used to obtain the tradeoff between ‘numerical accuracy’ and ‘numerical stability’ with the mass scaling factor of 5000 to ensure the neglected in effects of explicit FE simulation.

The detailed solutions involved in FE modeling can be found in literature (Li et al., 2007). Here especially the friction related issues and experimental evaluation of FE simulation are focused.

3.1. Friction formulations and modeling

In simulation of sheet metal forming process, the Coulomb law is generally chosen to represent the friction behaviors (Joun et al., 2009). Here an extended Coulomb model is used to describe the transmission of normal pressure force and tangential shear stress in tube bending. The concept of Coulomb law assumes no relative motion occurs if the tangential frictional stress is less than the critical stress, τ_{crit} , which is proportional to the contact normal stress, σ_n , in the form as Eq. (2).

$$\tau_{crit} = \min(\mu\sigma_n, \tau_{max}) \quad (2)$$

where μ is the CoF that assumed that the CoF has no relationship with the slip rate and pressure force according to the TCT.

The stick/slip calculations determine when a point transfers from sticking to slipping or from slipping to sticking. The Coulomb model includes an additional limit, τ_{max} , which is user-specified and equals to initial yield stress of tube materials. If the equivalent stress is at the critical stress, τ_{crit} , slip between tube and dies can occur; otherwise, the tube and dies remain sticking contact state. In addition, the friction is assumed isotropic, thus the direction of the slip and the frictional stress coincide.

By the TCT, once the CoF was assigned in FE simulation, without considering the lubricant flow under pressure force, the value of CoF on each interface remains constant throughout the bending process, though the contact forces on various interfaces are different as shown in Fig. 7. The static CoF is assumed to be equal to the kinetic one. The reference CoFs on different interfaces are listed in Table 2. As mentioned in the experiment, no relative slip should be ensured on tube–clamp die interface by tight clamping. Thus the CoF on this interface should be larger to satisfy the tight clamping conditions. In ABAQUS, so-called ‘‘rough’’ friction with CoF ∞ is available, where it is assumed there is no bound on the shear stress and thus no relative motion can occur as long as the surfaces are in contact. The rough friction is implemented with the Lagrange multiplier method. The kinematic or penalty method is used to enforce this constraint.

The ‘‘surface-to-surface method’’ is used to define the contact behaviors between tube and various dies, which allows finite sliding between the above surfaces except for tube–clamp die interface. Table 2 also shows the formulations of the mechanical constraints about different contact pairs. If the kinematic algorithm is used with hard tangential surface behavior, the relative motion in the absence of slip is always equal to zero; with the penalty algorithm,

the relative motion in the absence of slip is equal to the friction force divided by the penalty stiffness.

3.2. Indices for evaluating the bending deformation of RDB

Several indices are proposed to evaluate the bending deformation correspondingly.

It is regarded that the wrinkling near the tangent point as general compressive instability in RDB. The difference between maximum tangent compressive stress and corresponding tangent tensile stress is proposed to represent the wrinkling possibility from the stress point of view (Li, 2007) as Eq. (3).

$$I_w = |\sigma_{maxc}| - |\sigma_{maxt}| \quad (3)$$

where σ_{maxc} is the maximum compressive stress at the inner side of tube; σ_{maxt} is the maximum tangent compressive stress at outer side of tube.

The larger I_w means increased wrinkling tendency. The stress difference is calculated within the bending angle 30° , due to the fact that the wrinkling phenomenon only occurs at the initial bending stage.

The wall thickness changing and cross-section deformation are another critical issues dealing with bending limit and forming quality. The wall thinning and thickening can be represented by Eq. (4)

$$I_t = \frac{t - t'}{t} \times 100\% \quad (4)$$

where t is initial thickness; t' is the minimum or maximum thickness after bending.

Due to the boundary constraints shown in Fig. 8, the tube is constrained in transverse direction by bend die groove and under free deformation conditions in vertical direction. Thus in RDB, the cross-section deformation can be determined by the changing ratio

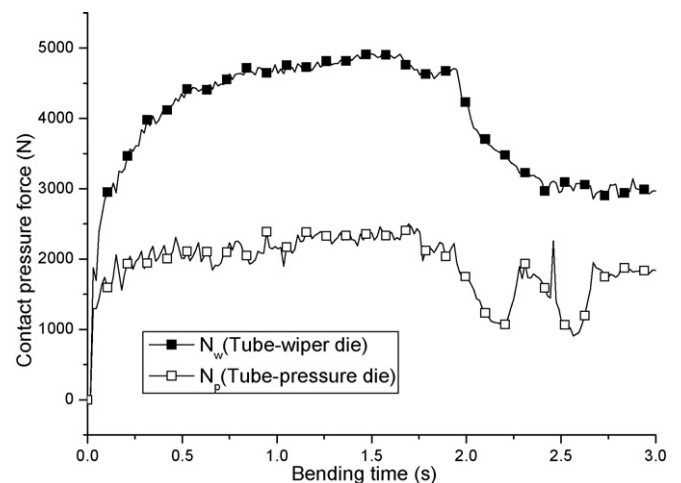


Fig. 7. The history curves of contact pressure force between tube and tools.

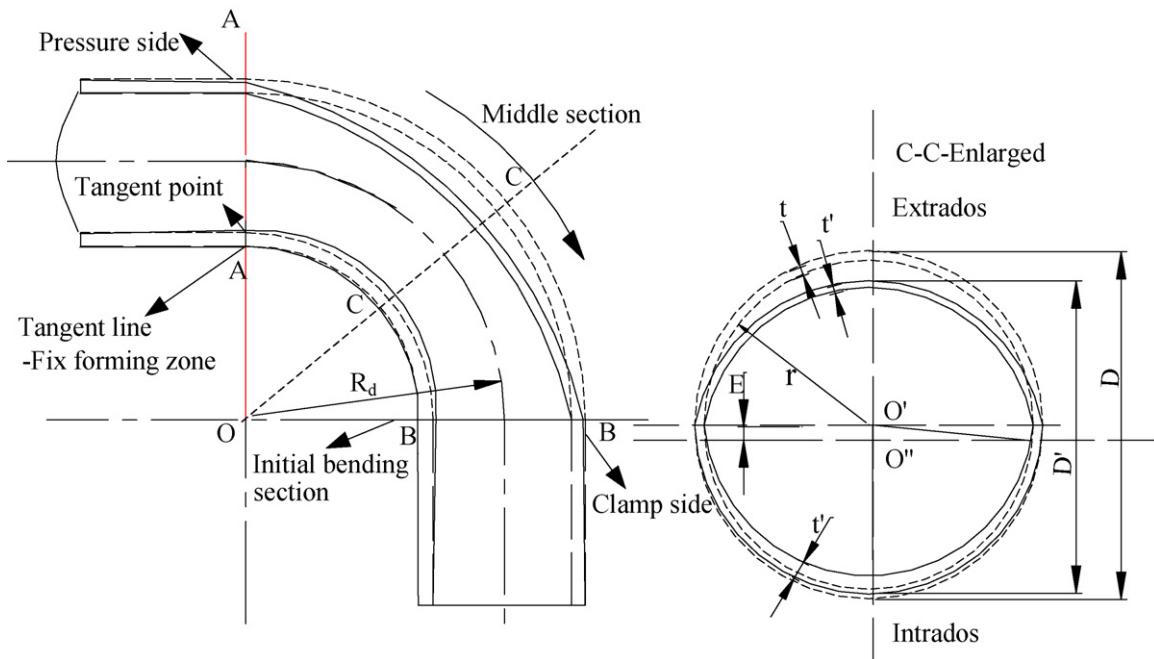


Fig. 8. Illustration of wrinkling region and wall thinning and cross-section deformation.

of the vertical magnitude of the cross-section as Eq. (5).

$$I_d = \frac{D' - D}{D} \times 100\% \quad (5)$$

where D is tube initial outer diameter; D' is the cross-section length in the vertical direction after bending.

3.3. Experimental evaluation of FE simulation

The verification of the FE modeling has been conducted in literature (Li et al., 2010). Here, by changing the lubricant conditions of tube–pressure die interface, the FE results are compared with the experimental ones to further validate the FE simulation of RDB. The forming conditions: the PLC (programmable logic controller) tube bender (W27YPC-63) is used. The bending specifications: Al-5052O 50 × 1 (diameter D × wall thickness t) under small R_d/D of 2.0. Table 3 shows the detailed forming conditions. The tools are made of steel-45#. The lubricant is S980B. The friction condition for tube–pressure die interface is DF and lubricant, respectively. The tribological conditions and the CoFs adopted in FE simulations on other interfaces are shown in Table 2.

Fig. 9 shows the comparison results in terms of wall thinning and cross-section deformation degrees. It is found that both the results present the bending characteristics of RDB of thin-walled tube, viz., both the maximum wall thinning degree and cross-section deformation are located near the clamp die. Also it is shown that under DF on tube–pressure die interface, the wall thinning and cross-section degrees can be improved effectively. The discrepancy between experimental results and numerical ones is that the actual assembling clearance between tube and various dies is a minor value, while there is no clearance on contact interface in FE modeling. Thus the overestimated results are obtained as shown in Fig. 9. Whereas, it is obvious that the FE results still coincide with the experimental curves. In terms of the maximum wall thinning degree, it is found that the relative error between experiment and simulation is less than 13.2% and the absolute error is about 4.3%; as for cross-section deformation, the relative error is less than 21% and the absolute error is about 1.1%. Thus, the developed FE model can be used to further explore the friction role in bending deformation of RDB.

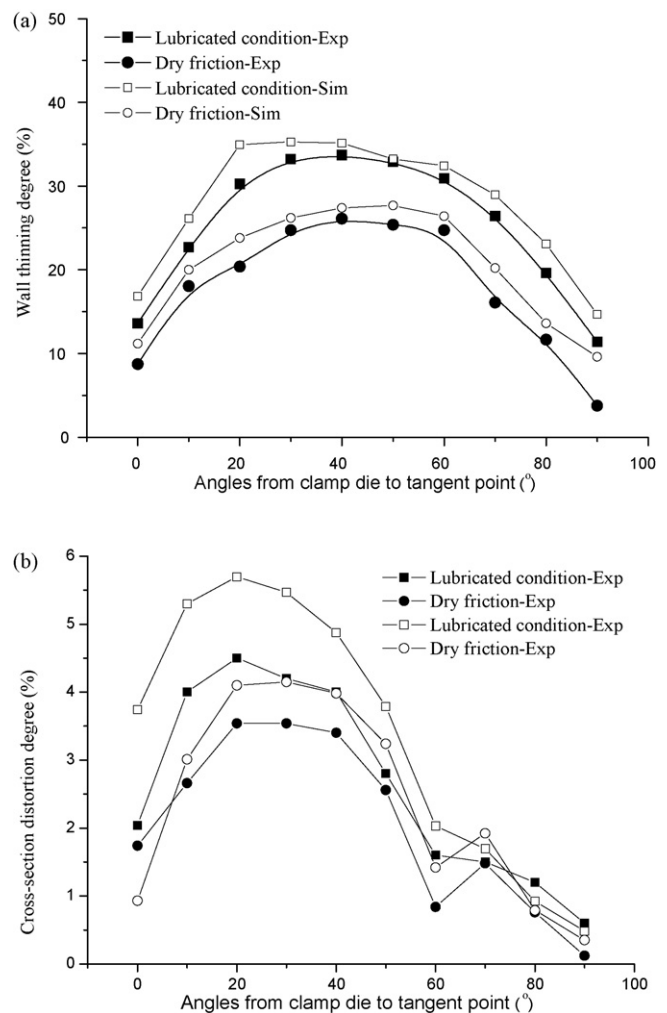


Fig. 9. Comparison of wall thinning and cross-section deformation degrees between FE and experiment under two different tribological conditions: (a) wall thinning; (b) cross-section deformation.

Table 3
Forming parameters for different tube bending specifications.

Specification of Al-5052O tube bending ($D \times t$)	50 × 1	50 × 1	38 × 1	38 × 1	70 × 1.5
Relative bending radius R_d/D (mm)	1.5	2.0	1.0	1.5	1.5
Assistant pushing speed of pressure die (mm/s)	60.0	80	30.4	45.6	84.0
Bending speed (rad/s)	0.8	0.8	0.8	0.8	0.8
Bending angle (rad)	$\pi/2$	$\pi/2$	$\pi/2$	$\pi/2$	$\pi/2$
Geometrical dimensions of mandrel	Diameter d (mm) Mandrel extension length (mm) Number of balls	47.6 6.0 3	47.6 6.0 2	35.6 6.0 2	35.6 6.0 2

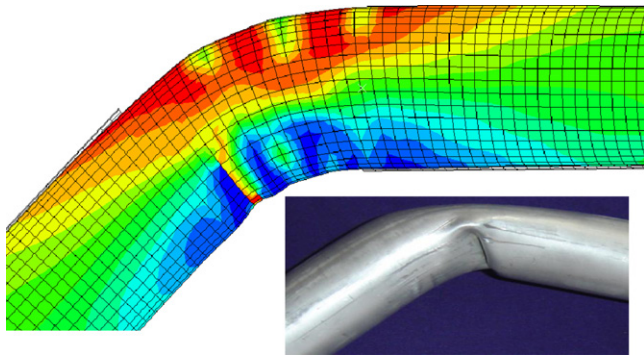


Fig. 10. The wrinkled tube with small CoF between tube and clamp die.

4. Results and discussion

An insight into the effect mechanism of friction in plastic bending deformation of RDB is provided quantitatively, and then an optimal strategy is proposed to positively control the lubricant conditions on different interfaces in RDB.

4.1. Friction role in bending deformation of RDB

The friction role in bending of RDB is studied from several aspects such as wrinkling, wall thickness change and cross-section deformation, respectively.

4.1.1. Primary friction condition for stable RDB of thin-walled tube

As mentioned in Section 2, the premise of RDB is that there is no relative slip between tube and clamp die. In the experiment, it is observed that, on tube–clamp die interface, under DF condition, there’s relative slip between tube and clamp die during tube bending and the wrinkling occurs near clamp die as shown in Fig. 10. While under tough DF condition, there is no relative slip on this interface, and the stable bending deformation can be accomplished with free wrinkling.

Thus the premise of achieving the stable bending deformation is that there is no relative slip on tube–clamp die interface. So the necessary tribological condition for stable tube bending is obtained, viz., tough DF should be applied to tube–clamp die to firmly draw the tube past the tangent point. Thus numerical study on the effect of friction conditions on other four interfaces including tube–wiper die, tube–mandrel, tube–pressure die and tube–bend die, on bending deformation can be conducted by changing the CoFs from 0.0 to 0.5, while the other CoF is applied based on Table 2. Without special declaration, the tube bending specifications are Al-5052O 38 × 1 × 57 under the forming conditions as shown in Table 3.

4.1.2. Effect on wrinkling instability

The wrinkling does not occur under all friction conditions at tube–wiper die. Fig. 11 shows that the tangent stress difference I_w decreases with the increasing of CoF on this interface. It indi-

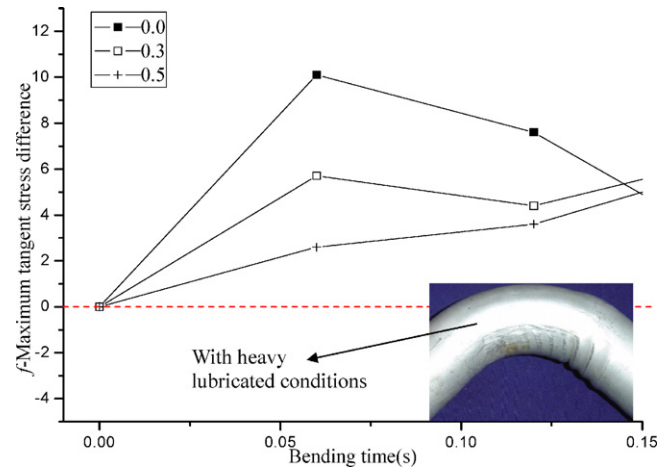


Fig. 11. Effect of friction between tube and wiper die on wrinkling.

icates that, the larger friction on tube–wiper die helps decrease the wrinkling tendency. The reason is that, the tangent friction stress at tube–wiper die induces the tensile stress at the intrados of tube, which causes the magnitude of the bending induced tangent compressive stress to be decreased. Thus the wrinkling tendency decreases. In the experiment, it is observed that, with heavy lubricated condition on this interface or polished tube, the wrinkling happens near the rear end of tube as shown in Fig. 11.

In addition, the wall thickening degree decreases with larger CoF on this interface (Fig. 12), which indicates that the larger CoF blocks the material’s forward flow near the tangent point. With larger CoF, the number of elements past the tangent point is less than that with smaller CoF. The number of elements with CoF 0.5 is less than that with CoF 0.2. However, it is experimentally found

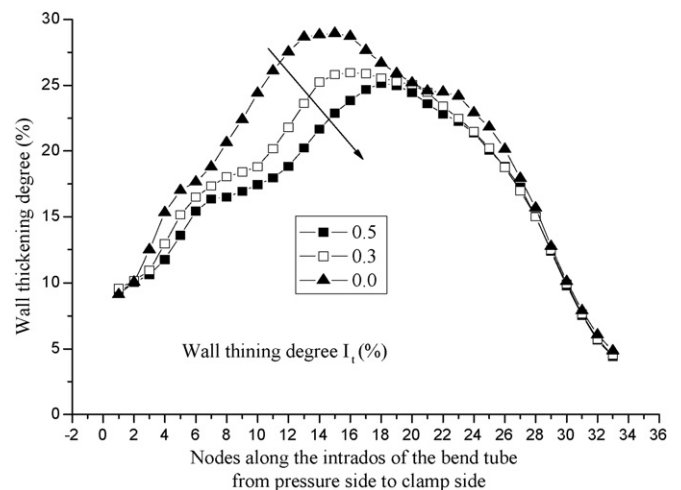


Fig. 12. Effect of friction between tube and wiper die on wall thickening from clamp side to tangent point.

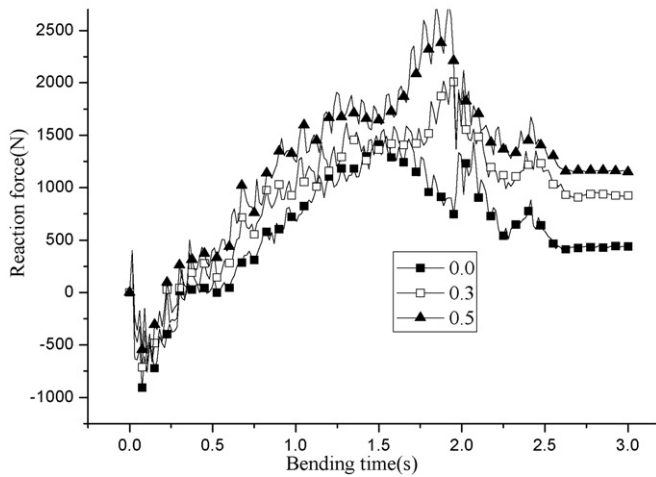


Fig. 13. Effect of friction between tube and wiper die on reaction force of bend die.

that, under DF condition, the tube flow behind wiper die is blocked by the friction force and the increased drag force of wiper die results in relative slip between tube and clamp die, which causes the wrinkling onset near clamp die. Fig. 13 shows that, the reaction force of bend die increases with larger CoF. Also the larger friction on this interface causes the abrasion/wear of wiper die. Thus taking into account the little significance of friction effect on wrinkling onset, the CoF on tube–wiper die interface should not be large.

The wrinkling does not occur when CoF on tube–mandrel interface is 0.0. While when the CoF is 0.3 and 0.5, the wrinkling occurs near clamp side and the ripples become more severe with larger CoF. That is because, when the friction force between tube and mandrel becomes larger, the drag force exerted by tube–mandrel friction increases, which prevents tube from moving forward and causes the contact condition of tube–clamp die to change from static state to kinetic one. Fig. 14(a) shows that, when the CoF increases from 0.0 to 0.25, the relative slip distance at tube–clamp die becomes larger progressively. While when the CoF on this interface exceeds 0.25, the relative slip distance increases sharply with larger CoF, which causes the wrinkling near clamp side. The severe wrinkling occurs with CoF of 0.5 on this interface. Meanwhile, with larger CoF, the tube materials cannot be drawn past the tangent point efficiently. Then excessive materials are piled up behind the wiper die, which results in the local wrinkling near the tangent point. Under DF condition, there are 10 elements flowing into the deformation region more than that with CoF 0.5. The reaction force of bend die becomes larger when the CoF increases on this interface. In the experiment, it is found that as shown in Fig. 14(a), DF condition aggravates the tools' wear and causes the scratch of tube surface.

On the contrary, Fig. 14(b) shows that, the tangent stress difference I_w decreases with larger CoF on tube–mandrel interface. That indicates the wrinkling tendency near the tangent point decreases with increasing of CoF on this interface. Similar with effect at tube–wiper die, the larger friction force at tube–mandrel results in decreased tangent compressive stress at the intrados, which reduces the general wrinkling risk near the tangent point. However, compared with that on relative slip distance, the friction effect on the general wrinkling instability is relatively little. The wall thickening degrees change little with CoF variation due to the relative slip on this interface with larger CoF, which further confirms that the friction has little effect on general wrinkling tendency on this interface. Thus it is thought that, the larger friction of tube–mandrel may cause decreased general wrinkling tendency near the tangent point but increased wrinkling risk near clamp side. The above

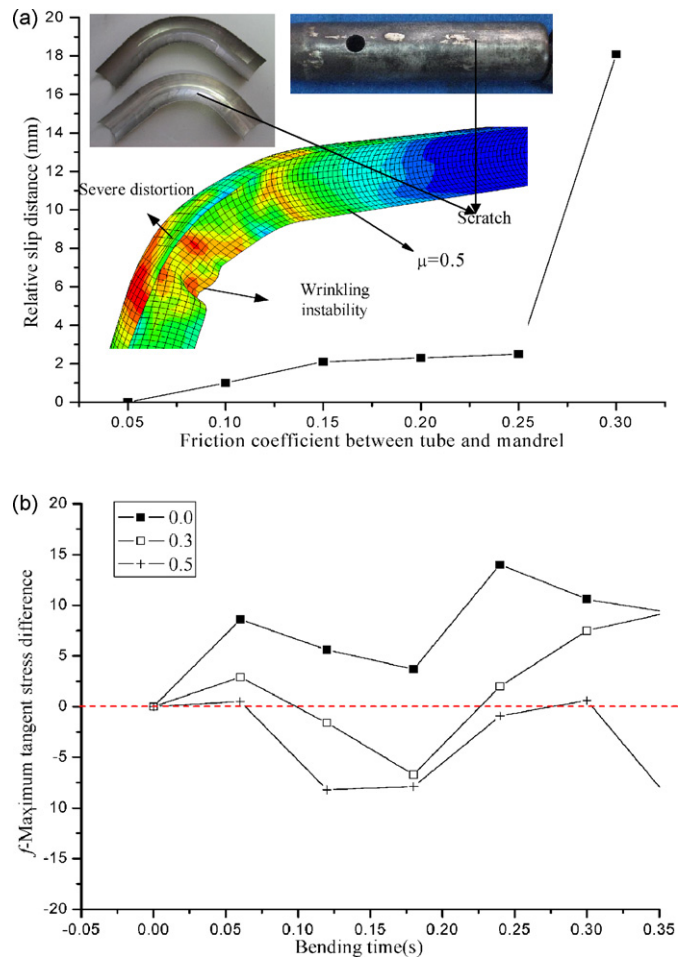


Fig. 14. Effect of friction between tube and mandrel on wrinkling (a) the relative slip between tube and clamp die; (b) the value of f with different CoFs.

influential laws on wrinkling are similar with ones of friction at tube–wiper die.

As for tube–pressure die, it shows that the wrinkling does not occur under various friction conditions. Fig. 15 shows that the tangent stress difference I_w increases with larger CoF on tube–pressure die interface. This indicates the larger CoF of tube–pressure die may increase the wrinkling tendency. Also it is found that the larger

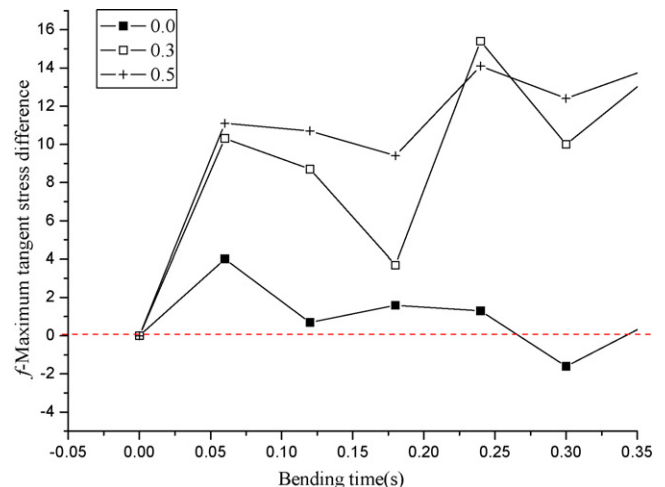


Fig. 15. Effect of friction between tube and pressure die on wrinkling.

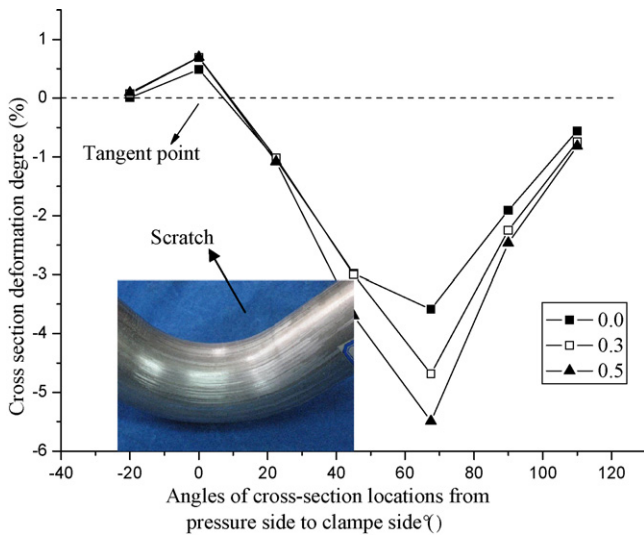


Fig. 16. Effect of friction between tube and pressure die on wrinkling.

CoF leads to the larger wall thickening, which further proves the above conclusion. While the larger CoF on this interface decreases the reaction force of bend die, which prevents the relative slip between tube and clamp die and thus avoids the wrinkling near clamp side.

For tube–bend die, the wrinkling does not occur under various friction conditions. It is found that the tangent stress difference increases with larger CoF on this interface. That is because, due to the characteristics of RDB, the materials are clamped and drawn past the tangent point, then the materials are deformed and sticking with the groove of bend die. If the CoF on this interface turns larger, the stable compressive deformation near the tangent point may be blocked and thus the instability occurs. But it is found the reaction force of bend die becomes smaller with increasing CoF on this interface.

4.1.3. Effects on wall thickness variation and cross-section deformation

Fig. 16 shows that, the larger friction on tube–wiper die interface results in more severe cross-section deformation as well as larger wall thinning and scratch of tube surface. The reason is that, with larger CoF on this interface, the tangent tensile stress at the extrados increases, which leads to more severe wall thinning I_t and cross-section deformation I_d . As to CoF on tube–mandrel interface, the similar conclusion is obtained with that at tube–wiper die. For tube–bend die interface, the friction on this interface has little effect on the wall thinning at the extrados, while the larger CoF on this interface reduces the I_d to some extent.

The friction role of tube–pressure die on I_t and I_d is also addressed. Fig. 17(a) shows that the larger CoF on this interface helps reduce both the I_t and I_d . The reason is that the larger friction on this interface improves the pushing assistant function of pressure die. The larger friction force reduces the tangent tensile stress at the extrados and helps push more materials into plastic bending regions. Also the relative slip between tube and clamp die and wrinkling near clamp die can be avoided effectively. As mentioned in Section 3.3, in the experiment, it is observed that, under lubricated condition on this interface, both the wall thinning and cross-section deformation degrees become severe, and the wrinkling occurs near clamp side due to the relative slip of tube–clamp die. For Al-5052O tube, even the crack occurs. While under DF condition, the stable bending deformation can be achieved. In addition, under lubricated and DF conditions, the moving distances of tube relative to wiper die are 140.4 and 149.2 mm, respectively. That

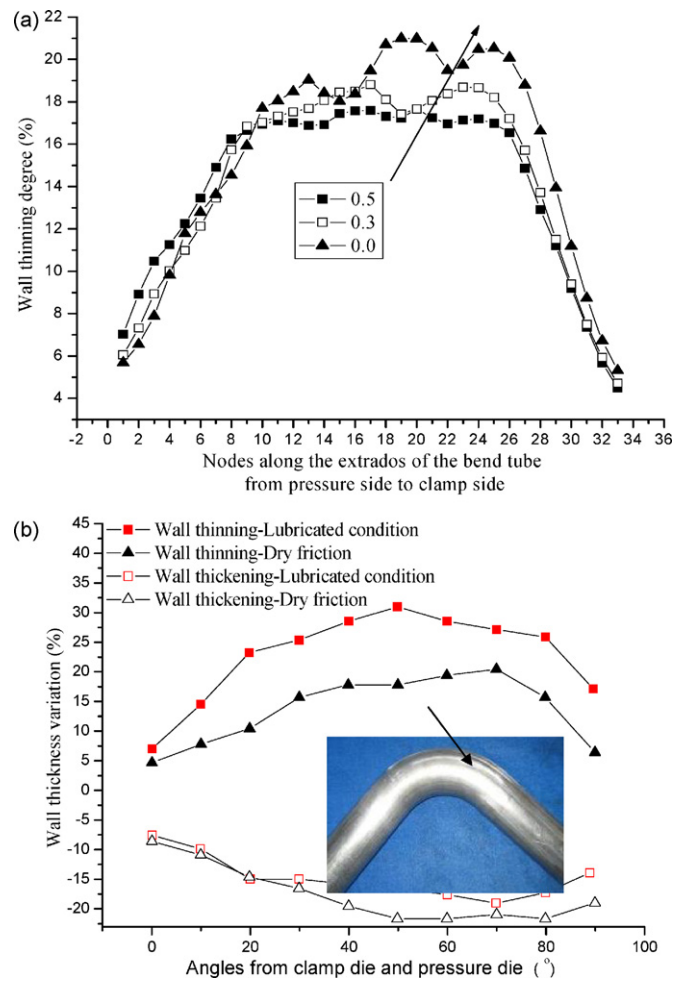


Fig. 17. Effect of friction between tube and pressure die on the wall thinning degree (a) Al-5052O 38 × 1 × 57; (b) Al-5052O 70 × 1.5 × 105.

implies that, more materials are pushed past the tangent point and under bending deformation.

4.2. Effect sensitivity of friction under small R_d/D

The effect significance of friction under small R_d/D of 1.0 and 1.5 is studied. The forming conditions are shown in Table 3. Fig. 18

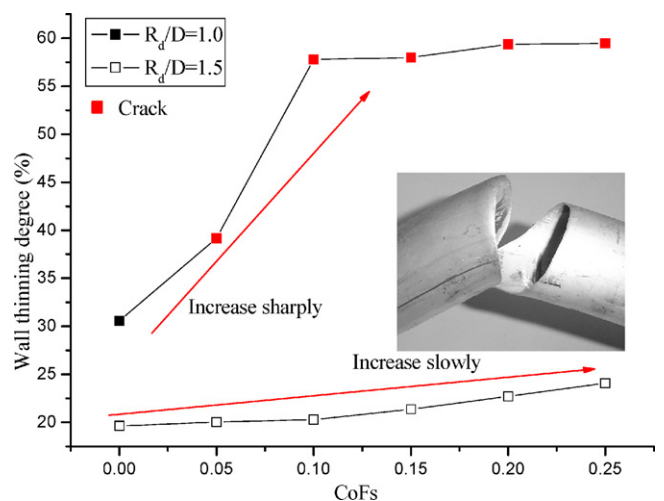


Fig. 18. Effect significance of CoF at tube–mandrel under different R_d/D .

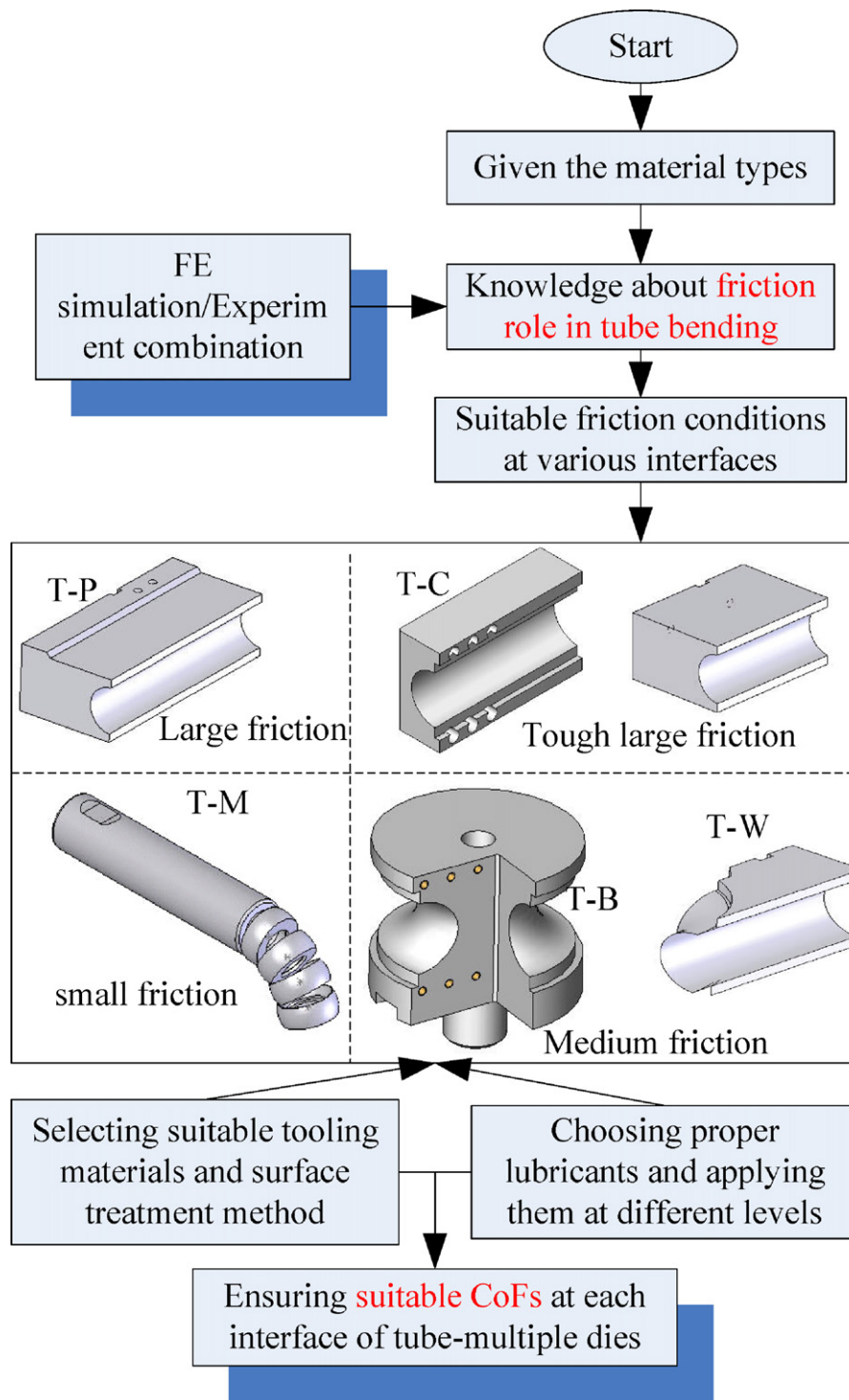


Fig. 19. The optimal application strategy of the tribological conditions in RDB.

shows that, under the bending radius of 1.0, by changing CoFs at tube-mandrel, the I_t becomes much more sensitive to the variation of CoFs. It is observed that, the crack occurs with the CoF of 0.05.

4.3. An optimal application strategy of the tribological conditions in RDB

Based on the above synthetical analysis, it shows that, by applying the proper friction conditions on five different interfaces with considering the interactive effects of friction on bending behav-

iors, the local or whole stress/strain states of tube can be improved and hence the multiple defects can be avoided or alleviated. Here, based on the understanding of the friction role in TWTB, an optimal strategy of friction application is proposed against different contact interfaces to ensure the suitable stress/strain distributions and precision bending parts (shown in Fig. 19).

For given tube materials, the proper tribological conditions should be adopted to achieve the desired friction levels for each friction interface. The related friction issues include whether to lubricate, to use suitable tooling materials for given tube mate-

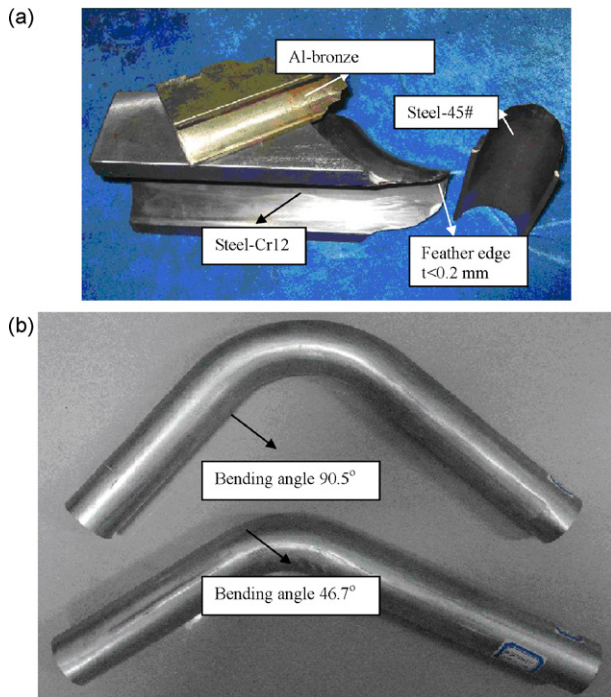


Fig. 20. Wiper die and experimental results for tube bending $50 \times 1 \times 75$: (a) different materials of wiper die for different tube materials; (b) experimental results with different bending angles.

rial and to apply proper lubricant on correct interface. According to TCT results, it is known that, for given tube materials, there are mainly two methods to change the values of the CoF and the tribological conditions: (1) to select proper tool materials and surface treatment method for given tube materials; (2) to choose appropriate lubricants and apply them at different levels (including DF condition). The detailed discussion is as follows.

- The friction on tube–clamp die interface (T–C) should be large to satisfy the necessary friction condition of RDB. With the smaller R_d/D , the required bending moment increases, which may cause relative slip between tube and clamp die due to small friction force. According to Eq. (2), to increase the friction on this interface, besides the increasing of the clamp force and DF application, some surface treatment methods such as knurling and coarse-sand-blasting should be adopted on the groove of clamp die to increase the CoF on this interface. The suitable CoF should be larger than 0.6. For relatively soft metal such as Al-alloy tube, a clamp insert should be used to further enhance the clamp force sometimes.
- It is known that the large friction of tube–wiper die (T–W) reduces the wrinkling tendency and increases the I_t and I_d . While the effect significance of friction on I_d is larger than those on both wrinkling and I_t . Furthermore, the wiper die is the vulnerable part with very thin feather edge (less than 0.3 mm) as shown in Fig. 20(a). During bending, there exists large normal pressure (about 4000 N as shown in Fig. 7) between tube and wiper die. Due to acute contact condition, the edge of wiper die may be worn heavily. Thus considering little friction effect on wrinkling and other defects, the tube–wiper die interface should be lubricated with a little oil to avoid abrasion and extend the life of wiper die. The suitable CoF on this interface should be 0.05–0.15. To reduce the friction on this interface and wear of tool, according to the TCT, the harder steel-45#, steel-Cr12 and Cr12MoV can be used to manufacture wiper die for Al-5052O tube bending, while the Al-bronze can be used as

Table 4
Roughness of the tube materials and bending tools for Al-5052O.

	Contact interface	Degree of roughness (Ra/ μm)	Surface treatment methods
1	Al-5052O tube	0.5	As received
2	Pressure die	1.8	Sand-blasting
3	Wiper die	0.6	Fine-sand-blasting
4	Mandrel	0.5	Fine-sand-blasting
5	Bend die	1.8	Sand-blasting
6	Clamp die	4.5	Coarse-sand-blasting

wiper die for 1Cr18Ni9Ti and TA18M tube bending (shown in Fig. 20(a)).

- Similar with friction condition on tube–wiper die interface, the friction between tube and mandrel (including flexible balls) (T–M) should be as small as possible. The suitable CoF on this interface should be 0.05–0.15. To reduce the friction on this interface, enough lubricant should be evenly pumped or hand-applied to the inside tube and mandrel surface. Furthermore, the steel-45#, steel-Cr12 and Cr12MoV can be used to make mandrel for Al-5052O tube bending, while the Al-bronze can be used for 1Cr18Ni9Ti tube. The special surface treatment methods such as fine-sand-blasting or hard chrome.
- The large friction should be applied to the interface between tube and pressure die (T–P), though the large friction of tube–pressure die may increase the wrinkling tendency to some extent. Relatively, it is noted that, the large friction on this interface can reduce I_t and I_d effectively. While the friction should not be increased too much as that of tube–clamp die. The reason is that, too much friction on this interface causes the tube outside surface to be scratched. The suitable CoF on this interface should be 0.35–0.45. Generally, DF condition satisfies the requirements of the stable bending without scratching tube outer surface.
- The suitable CoF on tube–bend die interface should be 0.35–0.45. The interface of tube–bend die (T–B) should be lubricated generally.
- For soft materials such as Al-alloy tube, the large friction condition may cause both outside and inside of the tube to be scratched. Hence, before bending process, the tube surface should be kept enough glazed. Sometimes, the tube surface should be coated to prevent scratching of rigid tools.
- The used lubricant shall not flow away under high contact pressure during RDB process; also, it should be easy to remove after bending and shall not stain the tube materials.

To verify the above optimal strategy of the friction treatment in RDB of thin-walled tube, the bending Al-5052O $50 \times 1 \times 75$ is conducted. The forming conditions as well as the friction conditions are shown in Tables 2 and 3. The Cr12MoV material is used to make the bending tools. The aviation oil is used as the lubricant. Both the fine and coarse-sand-blasting is applied to finish the different tools' surfaces, and the different roughness degrees are obtained as shown in Table 4. As shown in Fig. 20(b), by using the above optimal friction treatment, the stable and precise tube bending is achieved with allowed I_t ($I_t < 25\%$) and I_d ($I_d > -5\%$).

5. Conclusions

The tribological conditions against tube–tools interface are significant in affecting the stress/strain distributions and the deformation behaviors of the bending tube in RDB. Considering wrinkling, wall thinning and cross-section deformation, the knowledge about both sides (negative and positive effects) of friction role in bending behaviors of RDB is epistemologically revealed based on FE simulation/experiment combination method. The main results are summarized:

- (1) A TCT method is proposed to simulate the dynamic contact conditions of RDB and evaluate the dynamic friction behaviors of TWTB. The variations of the CoFs under different tribological conditions are estimated by the TCT. Among many influential factors, the type of lubricant, tube materials and tool materials are the decisive parameters related to the CoFs in RDB.
- (2) The friction should be designed for each interface at different levels. The necessary friction condition for stable bending is the clamp die and tube should be fastened tight. The larger friction at tube–wiper die and tube–mandrel cause more severe I_t and I_d ; considering little effect of friction on reducing I_w , the lubricants should be applied to these two interfaces. The larger friction on tube–pressure die interface reduces I_t and I_d effectively. Regarding little influence on increasing I_w , the larger friction should be applied on this interface with the tube surface not being scratched. The larger friction on tube–bend die interface can reduce I_d , and thus this interface should be treated with DF condition.
- (3) Based on the knowledge of friction role in affecting the bending deformation, an optimal strategy is proposed to apply the friction of RDB to improve the bendability effectively by two methods, viz., to choose suitable tooling materials and surface coating method, and to select proper lubricants and apply them to multiple interfaces at different levels, and also keep the friction condition as stable as possible.

By providing insight into the friction role in bending behaviors of RDB, the present study provides a guideline for applying the tribological conditions to establish the robust bending environment for stable and precise bending deformation of TWTB, thus the bending limit and quality of thin-walled tube can be improved by changing other processing parameters, especially for low-ductility materials.

Acknowledgements

The authors would like to thank the National Natural Science Foundation of China (No. 59975076 and No. 50905144), the National Science Found of China for Distinguished Young Schol-

ars (No. 50225518), State Key Laboratory of Materials Processing and Die & Mould Technology (No. 09-10) and NPU Foundation for Fundamental Research (No. JC201028) for the support given to this research.

References

- Bay, N., Olsson, D.D., Andreasen, J.L., 2008. Lubricant test methods for sheet metal forming. *Tribol. Int.* 41, 844–853.
- Hibbit Karlson and Sorensen Inc, ABAQUS Version 6.4, 2005.
- Joun, M.S., Moon, H.G., Choi, I.S., Lee, M.C., Jun, B.Y., 2009. Effects of friction laws on metal forming processes. *Tribol. Int.* 42, 311–319.
- Kim, H., Sung, J., Goodwin, F.E., Altan, T., 2008. Investigation of galling in forming galvanized advanced high strength steels (AHSSs) using the twist compression test (TCT). *J. Mater. Process. Technol.* 205 (1–3), 459–468.
- Li, H., 2007. Study on wrinkling behaviors under multi-die constraints in thin-walled tube NC bending. PhD Dissertation. Northwestern Polytechnical University, Xi'an, China.
- Li, H., Yang, H., Zhan, M., Sun, Z.C., Gu, R.J., 2007. Role of mandrel in NC precision bending process of thin-walled tube. *Int. J. Mach. Tools Manuf.* 47 (7–8), 1164–1175.
- Li, H., Yang, H., Zhan, M., Kou, Y.L., 2010. Deformation behaviors of thin-walled tube in rotary draw bending under push assistant loading conditions. *J. Mater. Process. Technol.* 210, 143–158.
- Lowery, S., 2008. Fact or friction? Understanding lubricant types is key to best selection. *Tube Pipe J.*
- Oliveira, D.A., Worswick, M.J., Grantab, R., 2005. Effect of lubricant in mandrel-rotary draw tube bending of steel and aluminum. *Can. Metall. Q.* 44, 71–78.
- Ramezani, M., Ripin, Z.M., Ahmad, R., 2009. Computer aided modelling of friction in rubber-pad forming process. *J. Mater. Process. Technol.* 209, 4925–4934.
- Tang, N.C., 2000. Plastic-deformation analysis in tube bending. *Int. J. Press. Ves. Pip.* 77 (12), 751–759.
- Trana, K., 2002. Finite element simulation of the tube hydroforming process-bending, preforming and hydroforming. *J. Mater. Process. Technol.* 127 (3), 401–408.
- Welo, T., Paulsen, F., Brobak, T.J., 1994. The behaviour of thin-walled aluminium alloy profiles in rotary-draw-bending—a comparison between numerical and experimental results. *J. Mater. Process. Technol.* 45, 173–180.
- Yang, J.B., Jeon, B.H., Oh, S.I., 2001. The tube bending technology of a hydroforming process for an automotive part. *J. Mater. Process. Technol.* 111 (1–3), 175–181.
- Yang, H., Zhan, M., Liu, Y.L., Xian, F.J., Sun, Z.C., Lin, Y., Zhang, X.G., 2006. Some advanced plastic processing technologies and their numerical simulation. *J. Mater. Process. Technol.* 177, 192–196.
- Yang, H., Yan, J., Zhan, M., Li, H., Kou, Y.L., 2009. 3D numerical study on wrinkling characteristics in NC bending of aluminum alloy thin-walled tubes with large diameters under multi-die constraints. *Comp. Mater. Sci.* 45, 1052–1067.